**Dalton Paper**

**Ref: B3126728**

# Supplementary Data

Lisa M. Wittick,[a] Keith S. Murray,*[a] Boujemaa Moubaraki,[a] Stuart R. Batten,[a] Leone Spiccia,[a] and Kevin J. Berry[b]

## Synthesis, Structure and Magnetism of new Single Molecule Magnets Composed of $Mn^{II}_2Mn^{III}_2$ alkoxo-carboxylate bridged clusters capped by triethanolamine ligands

### A more detailed Discussion of Magnetization versus Magnetic field studies

Magnetization isotherms (2 to 20 K; fields 0 to 5 T) were obtained on samples of **1** to **3** which were dispersed in vaseline mulls to prevent crystallite orientation anomalies (torquing).[18] These data were analysed in order to attempt to unambiguously determine the ground spin state, the size and sign of the zfs *D* term, and, perhaps provide information on any coupling between the $Mn_4$ clusters.

The magnetization isotherms at 2, 3, 4, 5.5, 10 and 20 K for cluster **1** are shown in Fig. 11. It can be seen that saturation does not occur in the highest fields even at 2 K, thus indicating that the ground state is not isolated energetically from higher states and/or is split by some other interaction such as zero field splitting. This is in agreement with the susceptibility analysis. The 2 to 4 K magnetizations become very similar in size above 2 T and reach ~15.5 Nβ at $H$ = 5 T, below the value of 17 Nβ expected for an isolated $S_T$ = 9 state, with a $g$ = 1.89. The 0 to 1 T region of Fig. 12 was investigated in more detail and gradual curvature was observed in the 2 to 5.5 K isotherms (not shown). This low field region also gave no evidence for any antiferromagnetic ordering transition, down to 2 K, of the type recently observed for a $Mn_4$ - hmp analogue.[10,11] There was no S - shaped behaviour in the $M$ vs. +/-2000 Oe plot typical of a metamagnetic transition. Thus any intercluster interactions are extremely weak in **1.** Included in Fig. 11 are the calculated $M$ values using the $g$, $J_{bb}$ and $J_{wb}$ parameters obtained for the 1 T field data analyzed using the tetramer model of eqns. (1) to (3). It can be seen that the 20 K data fit very well while, below 5.5 K, the low field region is fitted quite well whereas the higher fields give calculated values well above the observed data. This is because of zero field splitting and other effects, not included in the tetramer model.

As well as the $M$ vs. $H$ plots in Fig 12, the magnetization data for **1** are also plotted, in Fig. S1, as isofield 1, 2, 3, 4 and 5 T curves, in the $M$ vs. $H/T$ manner presented by Christou, Hendrickson *et al.*[7,8,11] Only the 2 to 4 K range is plotted to allow for thermal population of the ground state only, assuming this state is sufficiently isolated from the next higher state. The data clearly show that zero field splitting is occurring. The best fit for a $S$ = 9 state, with $D$ negative is shown in Fig. S1 using $g$ = 1.89 and $D$ = -0.21 $cm^{-1}$. An apparently better fit was obtained, as shown in Fig. S2 using $g$ = 1.89 and $D$ = +0.30 $cm^{-1}$, however this positive value of $D$ gives an unsatisfactory fitting of the 1 T data in the same temperature range. We see the reason for this below. Since, the frequency dependent AC susceptibility results, described later, are in agreement with $D$ being negative, a few pertinent points are now given on calculations of $M/H$ isotherms as a function of $D$, both positive and negative, for a $S$ = 9 state.

The calculations are very sensitive to the thermal populations of low lying Zeeman $m_S$ levels and to the splittings induced by the applied field. Calculations of the splittings of the energy levels in the perpendicular direction, at these low values of $D$ and in high magnetic fields, are more complex than those in the parallel field direction, as noted by Harris[21] for $S$ = 5/2 systems. The Hamiltonian used is given in eqn. (4), and powder averaging methods were used to calculate $M$ values.[20]

$$\mathcal{H} = D\boldsymbol{S}_z^2 + g\beta\boldsymbol{H}\bullet\boldsymbol{S} \qquad (4)$$

Calculated plots of $M$, for $D$ varying between -1 and +1 $cm^{-1}$, in fields 1 to 5 T, at 2 K and with $g$ = 1.89, are shown in Fig. 13. The $M$ values are unsymmetrical with respect to the $D$ value of zero, particularly at $H$ = 1 T. The isotherm is reasonably symmetrical for higher fields in the $D$ range +/- 0.3 $cm^{-1}$. These calculated plots were used to get a preliminary 'eyeball' value of $D$ and so horizontal lines of the observed $M$ values for **1** are given for $H$ = 1, 2, 3, 4 and 5 T, from which vertical lines to corresponding $D$ values can be obtained. The point made above in relation to the 1 T field can be understood since the observed 1 T magnetization crosses the calcualted 1 T isotherm at $D$ ~ -0.2 $cm^{-1}$ but barely crosses it in the positive $D$ region until ~ +0.7 $cm^{-1}$. The negative $D$ values also 'track' more sensibly at higher fields than do the positive $D$'s. Thus, we strongly favour a negative $D$ for **1** despite the apparent better fit given for positive $D$ in Fig. S2. Nevertheless, our analysis shows that some other effect, as yet undefined but possibly involving weak inter-cluster coupling, is playing a part in the magnetization results. High field EPR measurements, made at different temperatures, would help to unambiguously confirm the sign and size of $D$[7,8], but we do not have such facilities. These uncertainties did not occur, as far as can be ascertained, in the similar zero field splitting analysis made on the $M$ vs. $H/T$ plots for the related pdmH and hmp clusters.[7,8,11] However, the more extensive $M/H$ isotherms (2 to

20 K and 0 to 5 T) of the kind displayed in Fig. 11 were not given. The cluster-cluster interactions are also different to those found here.

The *M/H* isotherm plots for the benzoate complex **2** are broadly similar to those just described for **1**. However, the 1 T isotherm, at 4 K or 2 K, could not be fitted to a positive *D* value and this can be seen from the analogous diagram (not shown) to that in Fig. 13 in which the observed magnetization did not cross the calculated plot for positive *D*. The best-fit of the *M* vs *H/T* isofield data used $g = 1.95$ and $D = -0.23$ cm$^{-1}$ and agreed well for $H = 3$ T but, as in **1**, showed poorer agreement for $H = 1$, 2, 4 and 5 T. This is not too surprising since the small energy separation to the $S = 8$ state means that thermal population of such higher states will be more marked in **2** and the 'isolated ground state' model of eqn. (4) is not really appropriate.

The *M/H* data for the propionate cluster **3** are different in detail to those for **1** and **2**. This is a result of the intercluster antiferromagnetic coupling noted in the $\chi_M$ data at very low temperatures. Thus, the *M* values, in fields of less than 2 T, are essentially a linear function of *H*, and much lower in magnitude at a particular *H* than for **1** and **2.** The *M* value, at 2 K and 5 T, is similar to those of **1** and **2** (*ca.* 16 Nβ) and is still increasing rapidly, thus being far from a saturation value in this high field/low temperature region. There is a gentle S-shape in the 2 K data below 2 T, perhaps indicative of antiferromagnetic to metamagnetic behaviour arising from intercluster interactions. Indeed, plots of *M* vs *T* for fields of 0.01, 0.1, 0.5, 0.75, 1.0 and 1.5 T, show maxima in *M* at 2.5 K in fields above 0.5 T, indicative of antiferromagnetic coupling (Fig. 14). Heat capacity measurements would be required to see if this is an antiferromagnetic phase transition as was observed in $[Mn_4(hmp)_6Br_2(H_2O)_2]Br_2$.[10] To date, we have not achieved any satisfactory quantitative analysis of the magnetization data obtained on **3**.

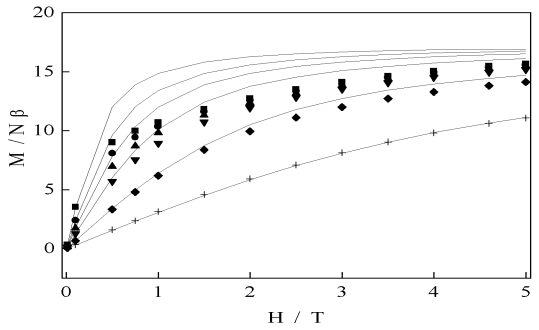


**Fig. 11** Magnetization isotherms for **1** at temperatures 20 (+), 10 (♦), 5.5 (▼), 4 (▲), 3 (●), 2 K (■). The solid lines are those calculated using the tetramer model with the *g* and *J* values given in the text, for 20 K (bottom) to 2 K (top).

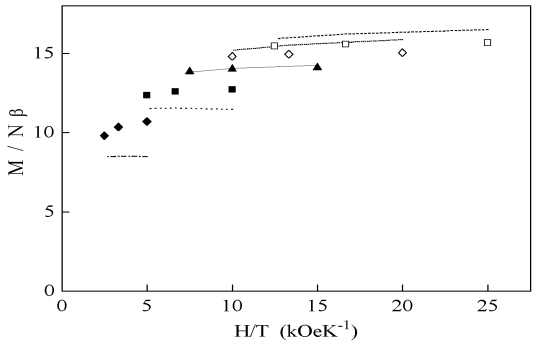


**Fig. S1** Isofield magnetization data (2 to 4 K) at fields of 1 (♦), 2 (■), 3 (▲), 4 (◊), 5 T (□). The calculated lines from eqn. 4 and $D = -0.21$ cm$^{-1}$, $g = 1.89$ are for fields of 1 (-·-·-), 2 (· · · ·), 3 (—), 4 (·····), 5 T (----).

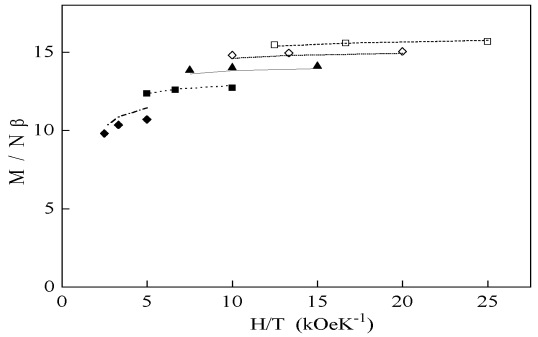


**Fig. S2** Isofield magnetizations for **1** as in Fig. 13 with calculated lines using $D$ = +0.30 cm$^{-1}$, $g$ = 1.89.

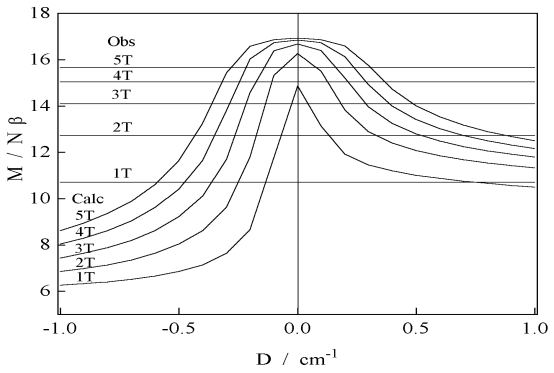


**Fig. 13** Calculated $M$ values at 2 K using $g$ = 1.89 and $D$ positive and negative (the curves should be smooth). Horizontal lines are the $M$ values observed in the fields given.

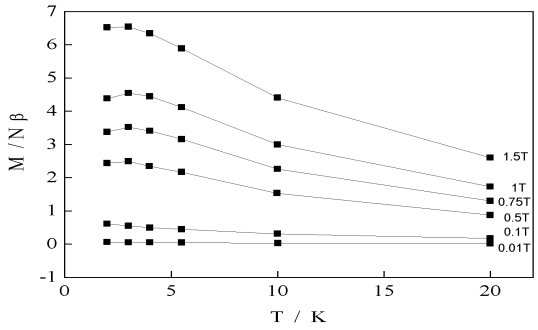


**Fig. 14** Observed $M$ values for cluster **3** in the fields given. The solid lines just join the points.

**Table S1a** Bond Valence Sum (BVS) Calculations[a] (Compound **1**)

| **Mn(1)** | **r** | **(r0-r)/B** | **s** |
|---|---|---|---|
| O(13) | 2.186 | -1.070 | 0.343 |
| O(23) | 2.426 | -1.719 | 0.179 |
| O(21') | 2.128 | -0.914 | 0.401 |
| O(14) | 2.199 | -1.105 | 0.331 |
| O(11) | 2.373 | -1.576 | 0.207 |
| N(1) | 2.396 | -1.443 | 0.236 |
| O(12) | 2.204 | -1.119 | 0.327 |
| | | | **2.024** |
| **Mn(2)** | | | |
| O(13) | 1.877 | -0.316 | 0.729 |
| O(23) | 1.989 | -0.619 | 0.539 |
| O(23') | 2.201 | -1.192 | 0.304 |
| O(21) | 1.907 | -0.397 | 0.672 |
| O(24) | 1.939 | -0.484 | 0.616 |
| N(2) | 2.384 | -1.492 | 0.225 |
| | | | **3.085** |
| | | | |

**Table S1b** Bond Valence Sum (BVS) Calculations[a] (Compound **2**)

| **Mn(1)** | **r** | **(r0-r)/B** | **s** |
|---|---|---|---|
| O(1) | 2.281 | -1.327 | 0.265 |
| O(7) | 2.305 | -1.392 | 0.249 |
| O(6') | 2.083 | -0.792 | 0.453 |
| O(4) | 2.409 | -1.673 | 0.188 |
| O(3) | 2.308 | -1.400 | 0.247 |
| N(1) | 2.377 | -1.392 | 0.249 |
| O(2) | 2.175 | -1.041 | 0.353 |
| | | | **2.003** |
| **Mn(2)** | | | |
| O(1) | 1.868 | -0.292 | 0.747 |
| O(7) | 1.962 | -0.546 | 0.579 |
| O(7') | 2.255 | -1.338 | 0.262 |
| O(6) | 1.912 | -0.411 | 0.663 |
| O(5') | 1.915 | -0.419 | 0.658 |
| N(2) | 2.316 | -1.308 | 0.270 |
| | | | **3.180** |
| | | | |

**Table S1c** Bond Valence Sum (BVS) Calculations[a] (Compound **3**)

| **Mn(1)** | **r** | **(r0-r)/B** | **s** |
|---|---|---|---|
| O(3) | 2.276 | -1.314 | 0.269 |
| O(6) | 2.288 | -1.346 | 0.260 |
| O(7') | 2.108 | -0.859 | 0.423 |
| O(5') | 2.376 | -1.584 | 0.205 |
| O(1) | 2.236 | -1.205 | 0.300 |
| N(1) | 2.383 | -1.408 | 0.245 |
| O(2) | 2.243 | -1.224 | 0.294 |
| | | | **1.996** |
| **Mn(2)** | | | |
| O(3) | 1.880 | -0.324 | 0.723 |
| O(6) | 1.952 | -0.519 | 0.595 |
| O(6') | 2.269 | -1.376 | 0.253 |
| O(7) | 1.910 | -0.405 | 0.667 |
| O(4) | 1.921 | -0.435 | 0.647 |
| N(2) | 2.393 | -1.516 | 0.220 |
| | | | **3.104** |
| | | | |

[a] H.H. Thorp, *Inorg. Chem.*, 1992, **31**, 1585

**Table S2** H-bond distances (Å) for Complexes **1**, **2** and **3**

| D – H…A | D – H (Å) | H…A (Å) | D…A (Å) | D – H…A (º) |
|---|---|---|---|---|
| 1 | | | | |
| O(3) – H(3A)…O(2)_$2 | 0.86(2) | 1.85(2) | 2.703(2) | 172(2) |
| O(3) – H(3B)…O(1) | 0.89(3) | 1.80(3) | 2.666(2) | 162(2) |
| O(14) – H(14C)…O(25)_$1 | 0.83(1) | 1.82(1) | 2.655(2) | 177(2) |
| O(22) – H(22)…O(2)_$3 | 0.89(3) | 1.85(3) | 2.730(2) | 169(3) |
| O(14) – H(14D)…O(3) | 0.87(2) | 1.96(2) | 2.793(2) | 158(2) |
| O(12) – H(12)…O(1) | 0.83(1) | 1.77(1) | 2.592(2) | 176(2) |
| O(11) – H(11)…O(3) | 1.00(3) | 1.76(3) | 2.737(2) | 165(2) |
| 2 | | | | |
| O(2) – H(2)...O(9) | 1.09(1) | 1.52(1) | 2.580(6) | 164 (8) |
| O(3) – H(3)...O(10) | 0.94(7) | 1.76(7) | 2.674(6) | 164(6) |
| O(8) – H(8)...O(9)_$2 | 0.84(2) | 1.91(4) | 2.685(8) | 153(8) |
| 3 | | | | |
| O(8) – H(8A)…O(12) | 0.84 | 2.03 | 2.851(6) | 166.7 |
| O(1) – H(1A)…O(8)_$2 | 0.92(5) | 1.75(5) | 2.666(6) | 171(5) |

For **1**:$1 = [-x+1, -y+1, -z], $2 = [-x+2, -y, -z+1], $3 = [-x+2, -y+1, -z+1]; For **2**:$2 = [-x, y, -z+1/2]; For **3**:$2 = [x+1, -y+1/2, z+1/2]